applied sciences

MDPI

Article

Dynamic Simulation of a 5 Degrees of Freedom Rotor Dropping on a Protective Bearing

Xiao Yu *, Jianggui Han and Tingfeng Ming

College of Power Engineering, Naval University of Engineering, Wuhan 430030, China; hanjianggui@hotmail.com (J.H.); hgming@126.com (T.M.)
* Correspondence: yuxiao9886@163.com

Abstract: In the magnetic suspension bearing system, the protection bearing, as its key component, plays a role in supporting the safe operation of the drop rotor after the failure of the magnetic suspension bearing, to protect the whole system from damage. Based on a multi-body dynamics simulation, this paper studied the characteristics of the protection bearing, such as the speed fluctuation of the rotor and the bearing inner ring, and the contact force between the rotor and the protection bearing when the 5-DOF rotor fell on the protection bearing. By adjusting the friction coefficient, the initial speed of the rotor, and other parameters, the movement process of the rotor falling in the protection bearing was studied. By comparing the speed fluctuation and contact force of the rotor and the bearing inner race, the influencing factors and rules of the impact of the rotor falling on the protection bearing were analyzed and summarized.

Keywords: protection bearing; rotor drop; dynamics simulation modeling; multi-body dynamics simulation

check for updates

Citation: Yu, X.; Han, J.; Ming, T. Dynamic Simulation of a 5 Degrees of Freedom Rotor Dropping on a Protective Bearing. *Appl. Sci.* **2024**, *14*, 2837. https://doi.org/10.3390/app14072837

Academic Editor: Jean-Jacques Sinou

Received: 9 February 2024
Revised: 17 March 2024
Accepted: 20 March 2024
Published: 28 March 2024

Copyright: © 2024 by the authors. Licensee MDPI, Basel, Switzerland. This article is an open access article distributed under the terms and conditions of the Creative Commons Attribution (CC BY) license (https://creativecommons.org/licenses/by/4.0/).

1. Introduction

In the active magnetic bearing (AMB) system [1], as a key component of the AMB protection system, the protection bearing [2] plays a role [3] in temporarily supporting the rotor and protecting the whole system from damage after the failure of the AMB [4,5]. However, in actual working conditions, the traditional protective bearing is often unable to support the high-speed rotation of the rotor [6–8], and the huge vibration and impact caused by the drop will affect the reliability and safety [9,10] of the whole magnetic levitation system.

The technical problems of the five-degree-of-freedom rotor–protective bearing system are focused on the rotor dynamic response under the coupling influence of multiple complex working conditions and structural parameters in the dynamic process of rotor dropping to the protection bearing, and the processes of rotating speed fluctuation, rotor dropping track, protection bearing damage, and the like in the normal operation of the rotor are affected by the coupling influence [3,11] of multiple factors such as working conditions, structures, and the like. And as the internal structure of the protective bearing is complex, the dynamic modeling sometimes cannot facilitate the deep analysis of the motion state of the ball of the protective bearing, but it simplifies the rotor–protective bearing as a spring-damper system [12–14], which cannot truly reflect the internal motion of the actual bearing.

Therefore, this paper mainly uses the multi-body dynamics software to model the five-degree-of-freedom rotor–protective bearing system and simulate the rotor drop process [15], relying on the advantages of multi-body dynamics software [16], to establish a more realistic five-degree-of-freedom rotor–protective bearing system simulation model, to obtain more intuitive model and data, and to better summarize the law. At the same time, the future research trends and directions of rolling bearing slippage are prospected. On the other hand, the potentiality contribution of the article could be used in collaborative robotics [17]. The dynamic characteristics of rotor fall are analyzed theoretically through dynamic modeling

and multi-body dynamic simulation method, and the corresponding rules and conclusions are drawn, and then the optimization scheme is provided for the design and reliability of protective bearings.

In the second chapter, the dynamics simulation model of the five-degree-of-freedom rotor–protective bearing system is established. Firstly, several possible results of rotor drop in actual working conditions are introduced, and the mathematical model is established. Secondly, the five-degree-of-freedom rotor–protective bearing system model is established by the ADAMS multi-body dynamics software package (ADAMS VIEW 2020). The third chapter uses multi-body dynamics software to study the drop characteristics of the five-degree-of-freedom rotor, changes the initial drop speed of the rotor and the friction coefficient between the rotor and the protection bearing, summarizes the dynamic characteristics of the five-degree-of-freedom rotor falling on the protection bearing through the rotor speed and the inner ring speed of the protection bearing, and studies the performance of the contact force between the rotor and the bearing inner ring. The fourth chapter summarizes the findings of the article, so as to better play a guiding role in practical application.

2. Establishment of Dynamic Simulation Model for 5-Dof Rotor–Protective Bearing System

The process of the high-speed rotor falling on the protective bearing is very complicated. Theoretical research and an experimental analysis of this highly nonlinear dynamic process have been carried out at home and abroad. Observed from the radial direction, the motion forms of the rotor falling on the protective bearing can generally be divided into two types: cylindrical motion and conical motion. In actual experimental conditions, conical motion is the main motion mode when the rotor falls, but in the theoretical research, the rotor falls on the protective bearing. The form of motion on the protective bearing is mainly cylindrical motion. At the same time, when the rotor falls on the protective bearing in the form of cylindrical motion, the radial contact force between the two is five times that of when conical motion occurs. Using multi-body dynamics, the motion of the rotor falling on the protective bearing can be directly analyzed.

The motion process of the rotor falling on the protective bearing can be divided into four motion stages, namely free fall, impact collision, sliding, and free rolling. When the rotor starts to fall with a certain initial speed, the rotor is in the free fall stage before contacting the protective bearing; once the rotor contacts the protective bearing, the rotor begins to undergo multiple impact collisions within the gap circle and within the rotor and protective bearing. Under the action of friction between the rings, the rotor begins to slide on the inner ring of the protective bearing. Currently, the sliding includes two forms: sliding back and forth at the bottom of the gap circle and whirlpool sliding along the gap circle; finally, it continues to slide under the friction. Under the action of force, the speed of the rotor and the protective bearing at the contact point remains the same, and the roller performs pure rolling motion within the gap circle. But not every time the rotor falls on the protective bearing will the rollers undergo whirlpool sliding or pure rolling.

From this, a preliminary analysis of the fall trajectory of the rotor falling on the protective bearing can be carried out, but only a preliminary analysis of the protective bearing can be carried out. The analysis of the normal contact force and tangential friction force is not in-depth. Due to the imbalance of the rotor mass, medium influencing factors have a great impact on the dynamic response of the entire system. The main axis of inertia of the rotor, the geometric center axis, and the geometric center of the bearing may not coincide. When the rigid rotor falls freely on the protective bearing and starts to move arbitrarily in space, then considering the influence of the eccentric moment on the drop response of the rotor–protective bearing system, when the rotor mass center and the centroid do not coincide, the dynamic model of each state of the rotor drop process is further described in detail.

In this rotor–protective bearing system model, the rotor system in space has a total of five degrees of freedom, including axial degrees of freedom and radial degrees of freedom.

The radial four degrees of freedom are the degrees of freedom of translation along the x and y axes and the degrees of freedom around the axis. The degrees of freedom of rotation are those around the x and y axes, and the axial degree of freedom is the degree of freedom of rotation around the z-axis. Since the coupling effect between the radial degree of freedom and the axial degree of freedom is small and can be ignored, the radial degree of freedom and the axial degree of freedom can be studied as two independent subsystems when modeling the system.

Currently, the center of mass of the rotor is only affected by its own gravity. The distance between the protection bearing and the center of mass of the rotor is known. The rotor exerts radial support force and tangential friction force. The following equations can be listed for the force analysis of the four-degree-of-freedom rotor:

$$\begin{cases} m\ddot{x} = F_{ta} + F_{tb} \\ m\ddot{y} = F_{na} + F_{nb} - F_G \\ J_x\ddot{\theta}_x - J_z\omega\dot{\theta}_y = F_{rb}l_b - F_{ra}l_a \\ J_y\ddot{\theta}_y + J_z\omega\dot{\theta}_x = F_{ta}l_a - F_{tb}l_b \end{cases} \tag{1}$$

The equation of motion of the rotor around the axis is:

$$J_z\ddot{\theta}_\omega = -F_{ta}R_r - F_{tb}R_r \tag{2}$$

When the rotor rotates by an angle around the center of mass, the following system of equations can be listed based on geometric relationships [18]:

$$\begin{cases} x_b = x_G - l_b \tan\theta_y \\ x_a = x_G + l_a \tan\theta_y \\ y_b = y_G + l_b \tan\theta_x \\ y_a = y_G - l_a \tan\theta_x \end{cases} \tag{3}$$

In this paper, the five-degree-of-freedom rotor–protective bearing system [19] is simulated by the ADAMS multi-body dynamics software package, and the working environment is selected as follows: (1) Set the coordinate system: in the ADAMS modeling environment, there is a coordinate system that the origin is fixed but can rotate with the model, which is the general coordinate system of the system. In addition, the system will automatically mark a marker point on the center of mass of the rigid body, and use Cartesian coordinates according to the actual modeling needs. (2) Unit system selection: the ADAMS/view unit system has MMKS, MKS, CGS, and IPS, and this paper uses the basic unit MMKS, that is, the unit mm, mass kg, force N, and time s. (3) Set the characteristics of the object: The mass and moment of inertia of the component designed according to the actual size are automatically calculated by the system, but not designed according to the actual size. The mass and moment of inertia can be customized. (4) Solver setting: when solving the contact collision problem, based on the BDF rigid integration program, the GSTIFF algorithm with variable order, variable step size, and variable coefficient is adopted, and the SI2 integrator with stable glue is selected to solve the discontinuous problem.

For the whole bearing model, the constraint relationship between each part of the bearing is divided as follows: (1) the outer ring of the bearing is fixed with the base, so the outer ring is set as a fixed pair to fix the bearing on the base; (2) set a contact pair among a rolling body in that protective bearing, an inner ring raceway and an outer ring raceway, wherein the contact set is the key of the whole modeling process, the contact stiffness, the damping and the contact coefficient need to be set in the contact setting, and the friction contact is set at the same time; (3) a contact pair is arranged between the inner ring of the bearing and the rotor, and the contact stiffness, damping, contact coefficient, friction coefficient, and the like also need to be set; and (4) the axial force is ignored, and a plane pair is arranged between the rotor and the ground so as to axially restrain the rotor.

Using the ADAMS multi-body dynamics simulation software package to simulate the rotor–protective bearing system, the most important thing is the establishment of the model and the reasonable setting of parameters. In ADAMS, there are two ways to define contact: one is based on the Impact function, and the other is based on the recovery coefficient method. The Impact function is more applicable and accurate. It uses the contact stiffness coefficient and damping coefficient to calculate the impact force. This function is used to calculate the contact force in the model simulation in this paper.

When the two cylinders are in contact, use the solver to calculate the contact force between the two cylinders according to the Impact function [20]. When the position relationship of two contact objects is different, the expression of Impact function is different, which is a piecewise function, and the occurrence [21] of contact is determined by calculating the penetration depth s_0:

$$s_0 = R - r \tag{4}$$

$$F = \begin{cases} 0 & s \le s_0 \\ k(s - s_0)^e + c\dot{s} * STEP(s, s_0, -d_m, 1, s_0, 0) & s > s_0 \end{cases} \tag{5}$$

The STEP function is used to simulate the non-convergence of the calculation results caused by the sudden change in the contact damping. Due to the large impact in the rotor drop system, the penalty depth d_m is taken as 0.015 mm in the contact setting.

For the Impact function [22], the most important thing is to determine the contact stiffness coefficient, damping, and contact coefficient, because the internal contact force of the protective bearing and the contact force between the rotor and the inner ring of the protective bearing are in line with the basic conditions of the Hertz theory: (1) Assuming that the contact object only undergoes elastic deformation and obeys Hooke's law, due to the high hardness of the bearing steel, relative to the radius of the ball, (2) it is assumed that only the maximum surface compressive stress is considered, and the assumption is reasonable because the normal contact force on the contact surface of the rolling element is much greater than the tangential friction force. (3) Assuming that the semi-radial ratio of the contact surface size to the surface curvature of the contact object is very small, many previous experiments have proved that the results calculated according to this assumption are consistent with the experimental results, so the assumption is reasonable.

Therefore, the Hertz theory is generally used to calculate the internal contact force of the protective bearing, and this theory is used to calculate the contact stiffness coefficient in this paper.

According to the Hertz theory, the contact between the rolling element and the raceway in the protective bearing belongs to point contact. Under the action of load Q, the contact deformation between the ball and the raceway with the same material properties is [23]:

$$\Delta = e_\delta \sqrt[3]{(\sum \rho) Q^2} \tag{6}$$

where ρ is the principal curvature of the contact surface, e_δ is the Hertzian contact coefficient related to the principal curvature of the contact surface, which can be calculated from reference [24], and Q is the normal load on the contact surface. Therefore, the contact coefficient between the rolling element and the raceway is $k_b = {e_\delta}^{-3/2} (\sum \rho)^{-1/2}$, and the contact coefficient is 3/2 [25].

Because of the complexity of damping calculation, there is no reliable calculation method at present, and the experimental method is basically used to determine the damping. According to the experiment, the damping value is 1000 N·S/m.

The contact between the rotor and the inner ring of the protective bearing is also calculated by the Hertz theory. The contact problem between the rotor and the inner ring can be understood as the line–surface contact problem in Hertz contact. Since both the

rotor and inner ring of the bearing are cylinders with finite length, the contact deformation under load is [26]:

$$\Delta = 3.83 \times 10^{-5} \frac{Q^{0.9}}{l^{0.8}} \quad (7)$$

where l is the line contact width, and the contact width when the rotor contacts with the bearing inner ring is the bearing width, taken as $l = 20$ mm. It can be concluded that the contact between the rotor and the inner ring of the protective bearing is $k_r = 4.268 \times 10^{11}\ \mathrm{N/mm^{-10/9}}$, and the contact coefficient is 10/9. The experimental method is also selected for the value of contact damping, and the commonly used contact damping value of $1000\mathrm{N \cdot m/s}$ is selected [27].

It is also very important to set the contact friction. There are various methods to calculate the friction coefficient in the dynamic simulation of the bearing. In a previous study, it was found that the friction coefficient of 0.007 had a good effect, so the friction coefficient between the rolling body and the raceway was set to 0.007 in the modeling simulation.

After completing the rotor and bearing geometric model and constraint settings, the model needs to be inspected to find errors in modeling, such as invalid constraints, massless objects, unconstrained components, etc., and give warnings. After inspection, the five-degree-of-freedom rotor drop model has 63 objects, 118 contact settings, two fixed pairs, two plane pairs, and no redundant constraints. Set the drop clearance to 0.2 mm. The five-degree-of-freedom model is shown in Figure 1.

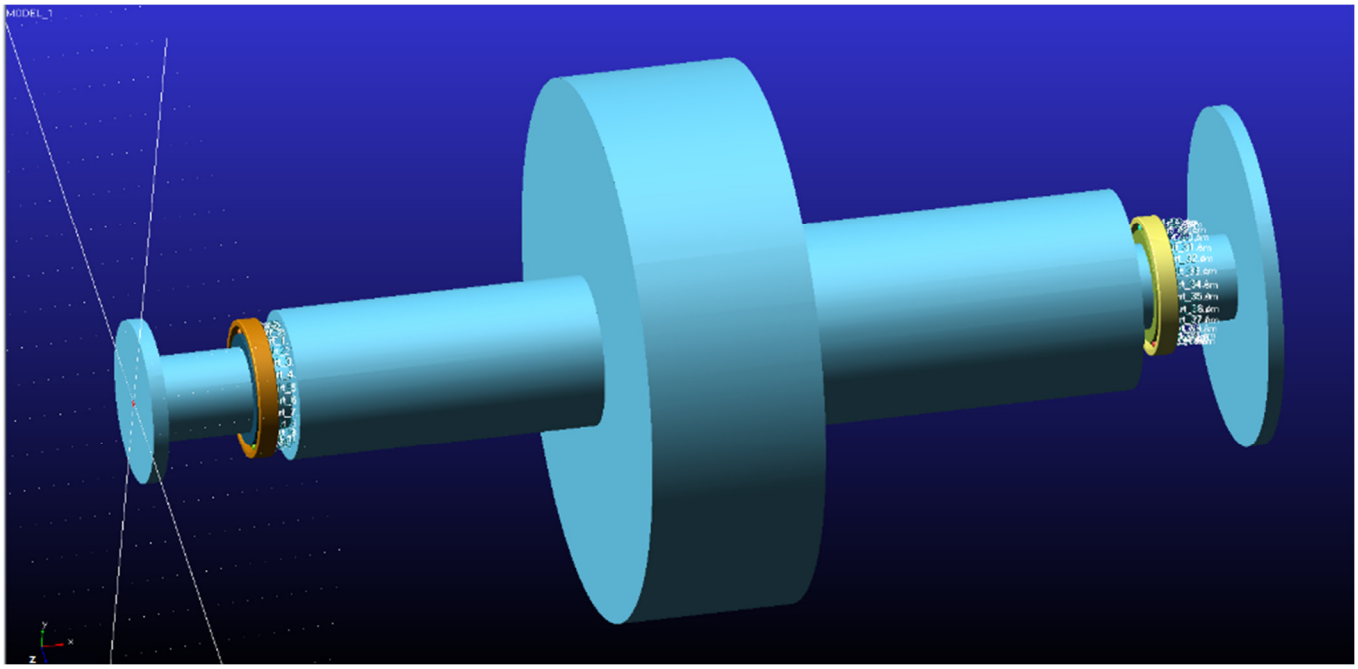

Figure 1. Schematic diagram of the 5-DOF rotor–protective bearing drop system modeling.

3. Characteristic Analysis of Dynamic Simulation Model of 5-Dof Rotor–Protective Bearing System

3.1. Simulation Study on Load Distribution of Protective Bearing

After completing the geometric parameter calculation of the protective bearing and rotor and the rotor–protective bearing system modeling in ADAMS, the protective bearing model needs to be verified in order to verify the accuracy of the model and parameter setting due to the complex internal structure of the protective bearing. According to the research on bearing load in the literature [8], when the inner ring of the protective bearing is subjected to radial load, the bearing area is general to its circumference, and each rolling body bears different loads, and its reasonable and radial loads are consistent. Assuming that the load on the inner ring of the protection bearing is known, the load on the maximum

bearing ball A is known, and the angle between the balls is known, then the force on each part of the bearing is known. The protective bearing model is shown in Figure 2.

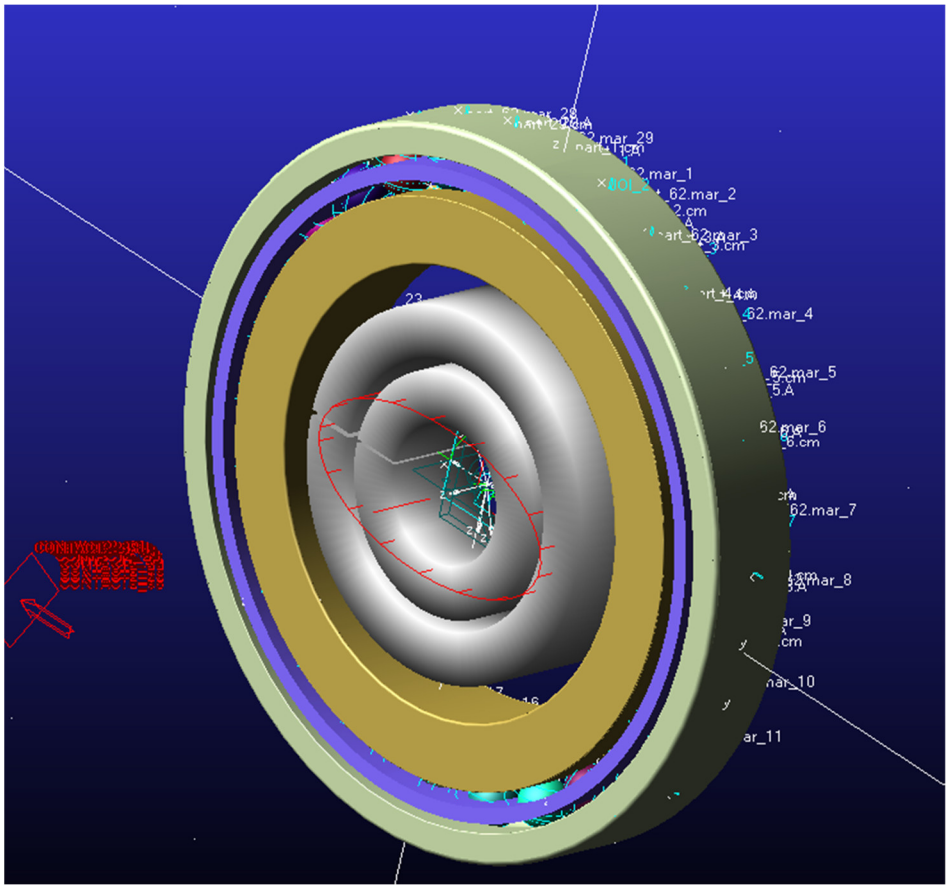

Figure 2. Schematic diagram of protective bearing modeling.

The load bearing of the bearing inner ring is borne by multiple balls, and the force balance can be obtained as follows [28]:

$$F_r = Q_A + 2Q_B \cos\gamma + 2Q_C \cos 2\gamma + \ldots \tag{8}$$

Satisfaction relationship between balls [29]:

$$\frac{Q_B}{Q_A} = \cos^{2/3}\gamma, \ \frac{Q_C}{Q_A} = \cos^{2/3} 2\gamma, \tag{9}$$

The relationship between the maximum load of the ball, the load on the inner ring, and the number of rolling elements Z can be simplified as follows [30]:

$$Q_A = \frac{4.36}{Z} F_r \tag{10}$$

Since the general rolling element inside the bearing has clearance, the actual bearing area is less than half of the bearing circumference, which is equivalent to fewer bearing balls under the same load, so the load borne by the maximum bearing ball in the actual situation is greater, and it is desirable to obtain:

$$Q_A = \frac{5}{Z} F_r \tag{11}$$

The dynamic verification of the established angular contact bearing is carried out in ADAMS. Firstly, a constant speed is set for the inner ring of the bearing, and a radial load is set in the direction of the *Y*-axis of the inner ring of the bearing. Because the rotor falls on the protection bearing at the speed of 6000 r/min in the working condition, and it is a five-degree of freedom system, the load on a single protection bearing is 5000 N. The simulation time is 0.1 s. The inner ring load is shown in Figure 3.

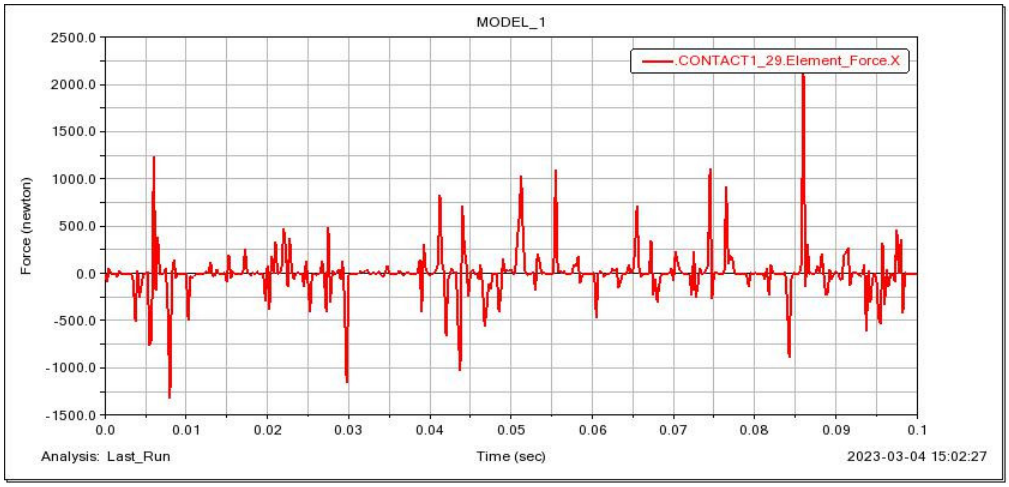

Figure 3. Load change in protection bearing inner ring.

Taking Z = 29, it can be concluded that the maximum bearing capacity of the ball is 946 N, and it can be seen that the ball load in the simulation results is basically about 1000 N, which verifies the correctness of the simulation model. The reason for the error may be due to the choice of a 10 μm clearance in the bearing modeling, and to the theoretical deduction of the calculation of the maximum bearing capacity of the ball; there are only two types: no clearance and clearance. The error may be caused by the difference in the clearance value.

3.2. Simulation Analysis of Rotor Speed Fluctuation during Rotor Dropping

To study the rotor speed fluctuation and the change in the inner ring speed of the protective bearing, an ADAMS simulation is carried out on the rotor–protective bearing system by changing the contact friction coefficient between the rotor and the protective bearing and the initial speed of the rotor. When the rotating speed is 6000 r/min, the results are as follows.

It can be seen from Figure 4 that the rotating speed of the rotor decreases in fluctuation under the action of the protective bearing, and it can be seen from Figure 5 that the rotating speed of the inner ring of the left and right protective bearings at this time is opposite to that of the rotor and increases in fluctuation. It can be found from the figure that the rotating speeds of the left and right protective bearings are not the same, which may be caused by the conical phenomenon when the rotor falls on the right and left protective bearings. But also related is that fact that the mass center of the rotor is not positioned at the midpoint of the left protective bearing and the right protective bearing, and so the system is not symmetrically distributed; by taking the mass center of the rotor as a center, the stress conditions of the left protective bearing and the right protective bearing are not symmetrical. Therefore, the rotor contact force on the left protective bearing is greater than that on the right protective bearing during the dropping process. According to Coulomb's law, with the increase in the normal contact force, the tangential friction force also increases, so the increase in speed of the left protective bearing is greater than that of the right protective bearing.

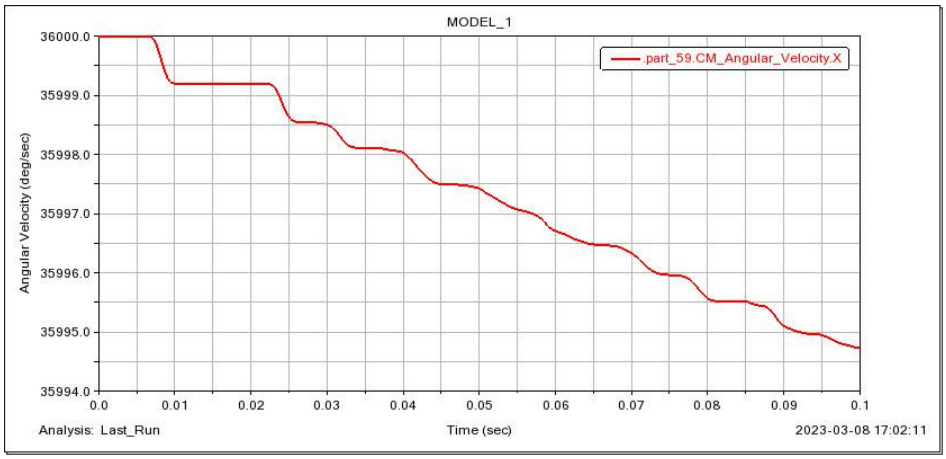

Figure 4. Simulation of rotor speed fluctuation when the initial rotor speed is 6000 RPM.

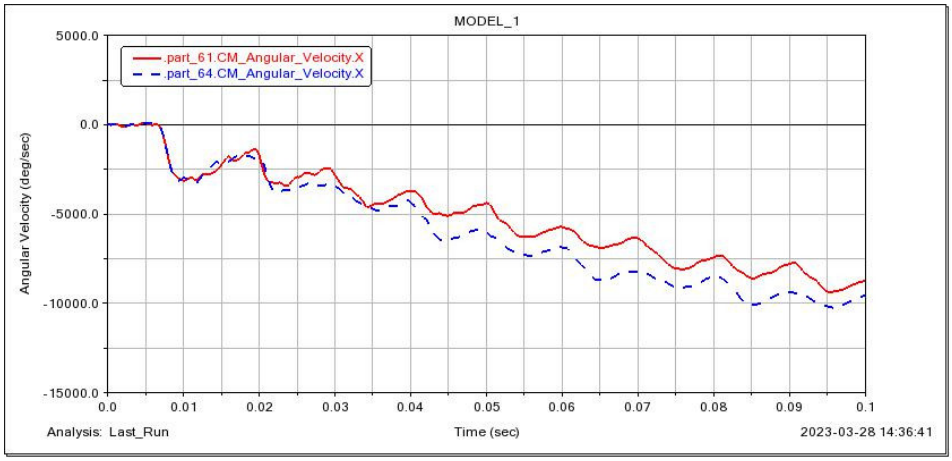

Figure 5. Simulation of bearing inner ring speed fluctuation when the initial rotor speed is 6000 RPM.

To study the speed fluctuation of the rotor and the protective bearing in the process of the rotor falling on the protective bearing in the ADAMS simulation, the contact friction coefficient between the rotor and the protective bearing is changed from 0.1 to 0.2, and the simulation time is 0.1 s. The results are shown in Figures 6 and 7.

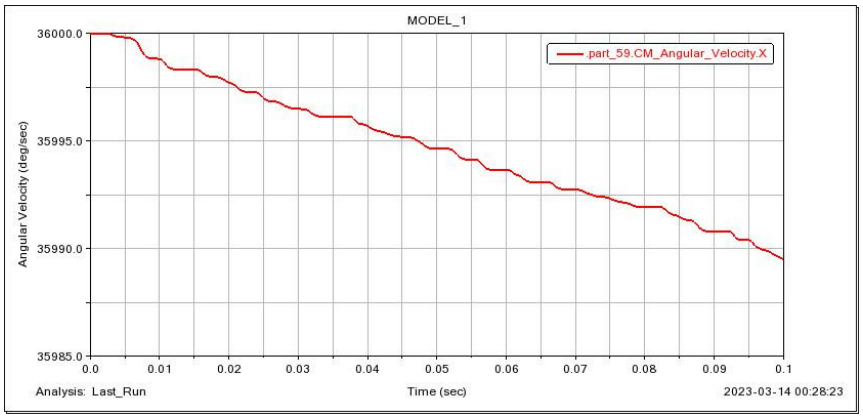

Figure 6. Simulation of rotor speed fluctuation with friction coefficient of 0.2.

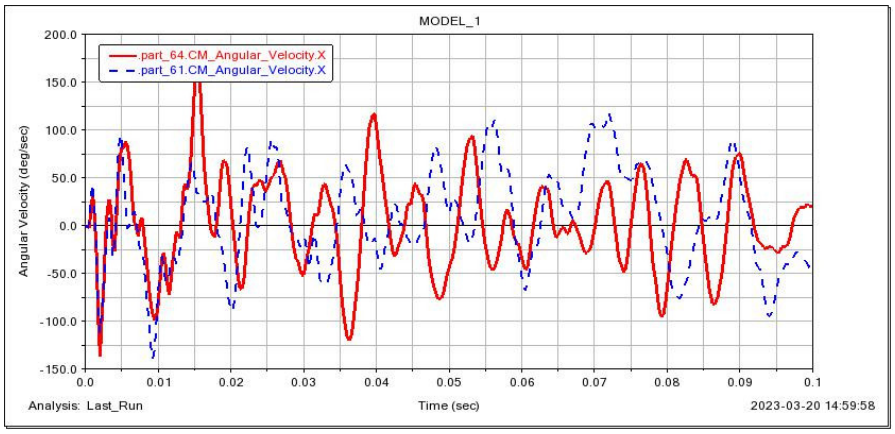

Figure 7. Simulation of bearing inner ring speed fluctuation with friction coefficient of 0.2.

The rotor speed drop speed increases, while the left and right protection bearing speeds increase, and the gap decreases. With the increase in the friction coefficient between the rotor and the protective bearing, the tangential friction between the rotor and the protective bearing increases, so the acceleration of the rotor increases, and the speed decreases more than when the friction coefficient is 0.1. However, the rotating speeds of the left and right protective bearings are still different. Currently, the rotating speeds of the protective bearings on both sides fluctuate. At the beginning, the speed fluctuations on both sides remain the same, and gradually begin to be asynchronous. It can be inferred that the rotor evolves from cylindrical motion to conical motion.

In order to further study the influence of the internal parameters of the protective bearing on the process of rotor dropping in the protective bearing, according to the speed fluctuation of the rotor and the protective bearing, the friction coefficient between the rolling element and the inner ring and the outer ring is studied by changing the friction coefficient between the rolling element and the raceway from 0.007 to 0.5 and carrying out an ADAMS simulation. The simulation time is 0.1 s, and the results are shown in Figures 8 and 9.

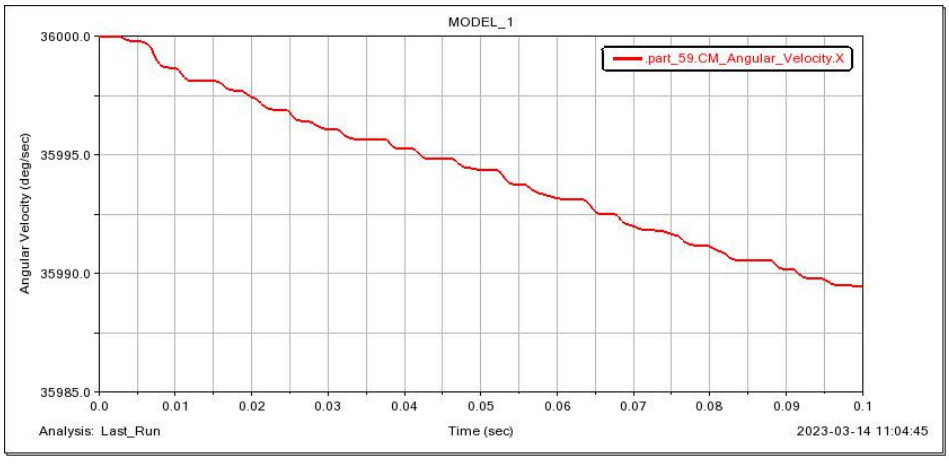

Figure 8. Simulation of rotor speed fluctuation with friction coefficient of 0.5.

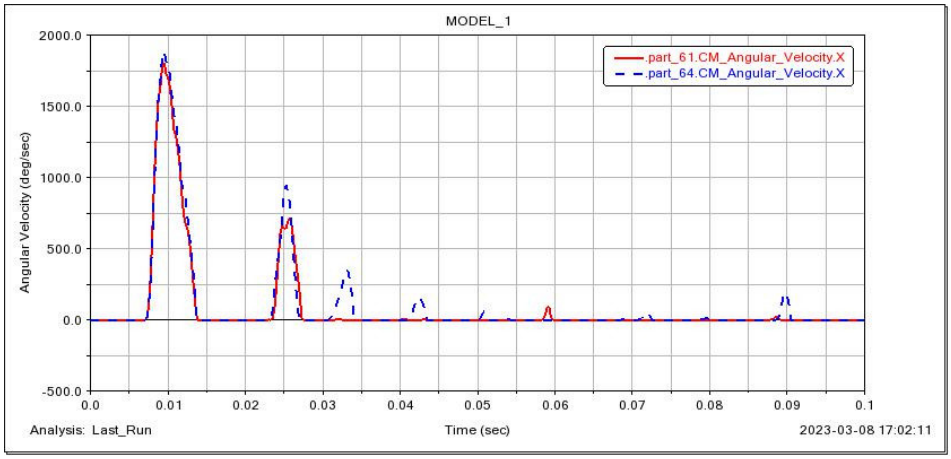

Figure 9. Simulation of bearing inner ring speed fluctuation with friction coefficient of 0.5.

It can be seen from the results that, compared with the previous results, there is not much difference between the rotor speed and the speed at the end of the simulation, but it can be found that the decline speed increases, while the speed of the inner ring of the protective bearing changes significantly. With the increase in the friction coefficient of the rolling elements in the protective bearing, because all the rolling elements act on the inner ring of the rolling bearing together, the friction force on the inner ring is very large. The inner ring keeps static most of the time, and the inner ring of the protective bearing will rotate only when the rotor falls on the protective bearing. At the same time, the rotating speeds of the left and right protective bearings are relatively consistent at the beginning, which indicates that the rotor does cylindrical motion in the inner ring of the protective bearing at the beginning, and the rotating speeds of the left and right inner rings are inconsistent at the later stage. It could be coning. Therefore, it can be found that the friction state of the inner rolling body of the protective bearing has a great influence on the motion state of the rotor in the falling process. In practical work, the damage to the system after the rotor falls can be improved by adding paint and other engineering methods to the inner rolling body of the protective bearing.

To study the influence of the initial speed of the rotor on the falling process of the rotor–protective bearing system, the initial speed of the rotor is set from 6000 r/min to 8000 r/min and ADAMS simulation is carried out. The simulation time is 0.1 s, and the results are shown in Figures 10 and 11.

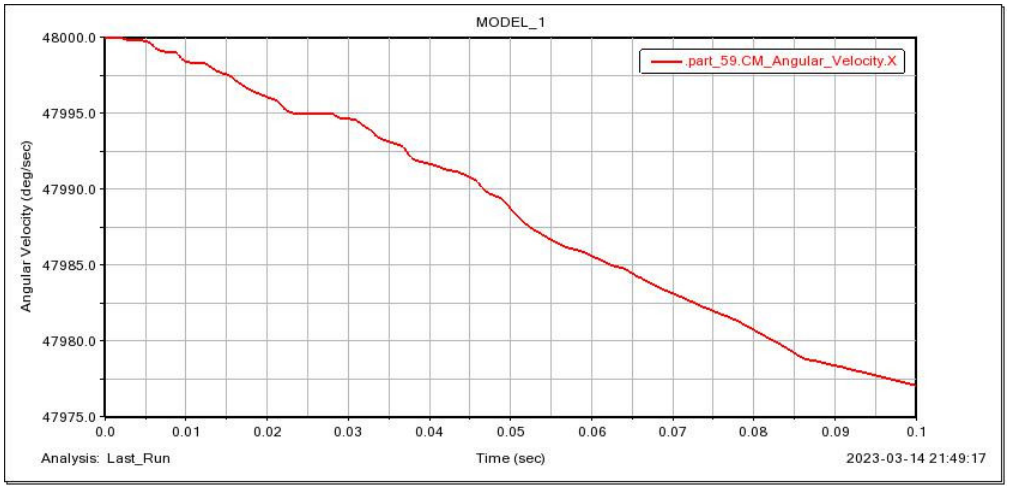

Figure 10. Simulation of rotor speed fluctuation when the initial rotor speed is 8000 RPM.

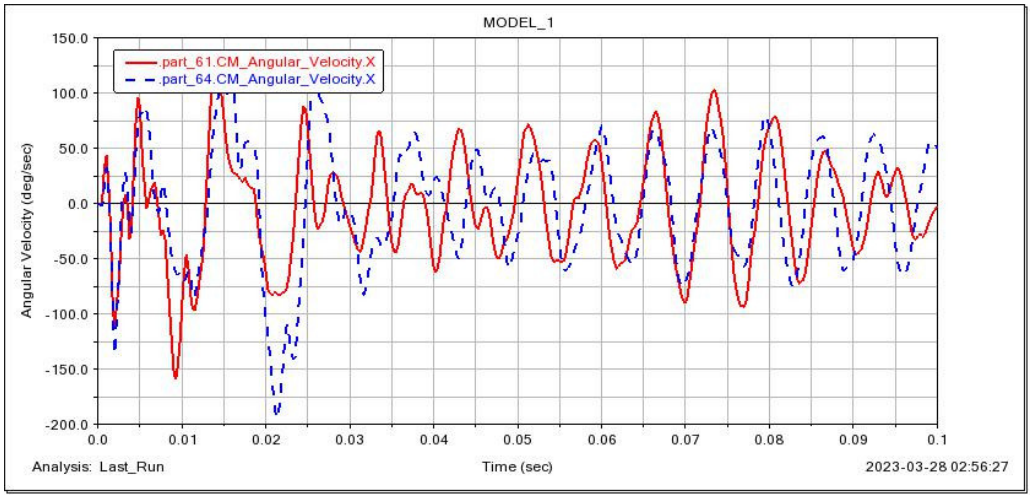

Figure 11. Simulation of bearing inner ring speed fluctuation when the initial rotor speed is 8000 RPM.

It can be seen from the results that after the initial speed of the rotor increases, the speed fluctuation of the rotor during the drop process becomes smoother, but the speed drops faster, and the inner ring speed of the protective bearing also increases, and the inner ring speeds of the left and right bearings increase asynchronously, and finally, the inner rings of the left and right protective bearings keep the same speed. It can be analyzed that when the initial speed of the rotor is very high, cylindrical motion occurs at the inner ring of the protective bearing at the beginning, and then it evolves into conical motion, and finally, it begins to do cylindrical motion again with the decrease in the speed.

3.3. Simulation Analysis of Contact Force Characteristics of Rotor Dropping

ADAMS can also be used to analyze the contact force. Through the post-processing function of ADAMS, the contact force between the rotor and the protective bearing during the rotor drop is studied. Compared with the numerical calculation, ADAMS has significant advantages. For the contact force characteristics of the rotor drop, the friction coefficient between the protective bearings and the initial speed are studied by changing the rotor. ADAMS simulation is carried out with 6000 r/min as the initial speed, and the simulation time is 0.1 s. The results are shown in Figure 12 below.

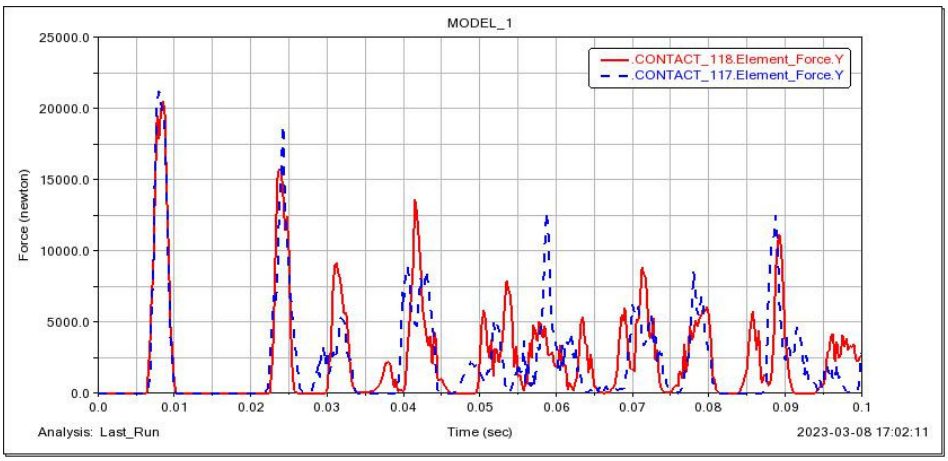

Figure 12. Simulation of contact force between rotor and bearing inner ring at initial speed of 6000 rpm.

It can be seen from Figure 12 that the rotor is in intermittent contact with the inner ring in the process of falling into the protective bearing. At the beginning, the impact force is strong and the impact interval is large, and then the impact force begins to attenuate and

the impact interval is also reduced. At the same time, it can be seen from the results that at the beginning, the contact forces on the inner rings of the left and right protective bearings are synchronous and similar in size. The contact forces on the left and right inner rings begin to be asynchronous with the drop process, so it can be analyzed that the rotor begins to fall in a cylindrical motion during the drop process, and the motion state of the rotor evolves from cylindrical motion to conical motion with the drop process.

In order to study the relationship between the initial speed of the rotor and the contact force between the rotor and the inner ring of the bearing in the process of rotor dropping, the initial speed of the rotor is set from 6000 r/min to 8000 R/min and ADAMS simulation is carried out. The results are shown in Figure 13 below.

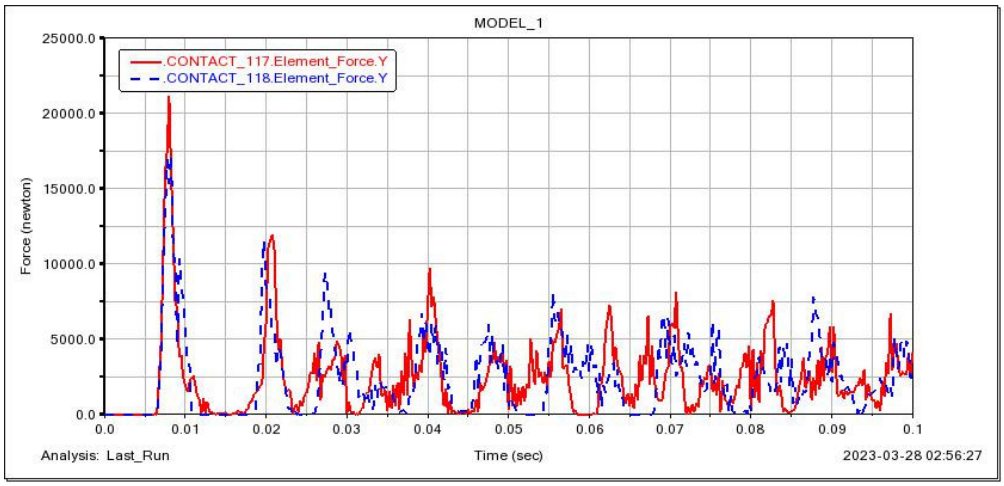

Figure 13. Simulation of contact force between rotor and bearing inner ring when the initial speed of rotor is 8000 rpm.

It can be seen from Figure 13 that with the increase in the initial speed of the rotor, there is no significant change in the contact force of the rotor falling on the inner ring of the protective bearing. At this time, the contact forces on the left and right protective bearings are synchronous at the beginning, and with the falling, the contact forces on both sides begin to be asynchronous. It can be analyzed that the rotor motion is cylindrical motion at the initial stage of the drop process, and then the contact force begins to be asynchronous, which can be inferred that the rotor evolves from cylindrical motion to conical motion. With the increase in rotating speed, the impact interval of contact force decreases and the occurrence of contact increases.

4. Conclusions

Multi-body dynamics simulation is performed on the five-degree-of-freedom rotor–protective bearing system. The contact between the bearing and the rotor is set according to the spring damping model. According to the main influencing factors that affect the rotor drop process, by changing the friction coefficient between the rotor and the bearing, For parameters such as the initial rotation speed of the rotor, multi-body dynamics simulation post-processing was used to study the effects of different parameters on the fluctuation of the rotor rotation speed during the drop process, the fluctuation of the rotation speed of the inner ring of the protective bearing, and the contact force characteristics with the bearing. The following can be concluded:

(1) Regarding the change in rotor speed after the rotor falls, the friction coefficient between the rotor and the inner ring of the protective bearing and the friction coefficient between the rolling element and the raceway of the protective bearing will affect the change in rotor speed. Increasing the friction coefficient will increase the frequency of rotor fluctuations, but there is little difference between the two friction coefficient changes on the rotor speed.

(2) The rotation speed of the inner ring of the protective bearing is affected by the friction coefficient between the rotor and the inner ring of the protective bearing and the friction coefficient between the rolling elements and the raceway of the protective bearing. The friction coefficient between the rolling elements and the raceway has a greater relative influence.

(3) After the rotor falls, the motion state gradually transitions from cylindrical motion to conical motion. As the friction coefficient increases, conical motion is more likely to occur.

Therefore, in order to reduce the impact force between the rotor and the inner ring, a coating can be used to protect the inside of the bearing in actual projects to reduce the impact between the rotor and the inner ring, thereby making the system safer and more reliable.

Author Contributions: Conceptualization, X.Y. and J.H.; methodology, X.Y., J.H. and T.M.; software, X.Y.; validation, X.Y., J.H. and T.M.; formal analysis, X.Y.; investigation, X.Y.; resources, J.H. and T.M.; data curation, J.H.; writing—original draft preparation, X.Y.; writing—review and editing, J.H. and T.M.; visualization, J.H.; supervision, J.H.; project administration, J.H.; funding acquisition, J.H. All authors have read and agreed to the published version of the manuscript.

Funding: This research received no external funding.

Institutional Review Board Statement: Not applicable.

Informed Consent Statement: Not applicable.

Data Availability Statement: The raw data supporting the conclusions of this article will be made available by the authors on request.

Conflicts of Interest: The authors declare no conflict of interest.

References

1. Wang, J.; Jia, X.; Zhang, K.; Xu, Y. Research on Dynamics of Magnetic Bearing Rotor Drop on Back-up Bearings. *China Mech. Eng.* **2022**, *33*, 2403–2413+2419.
2. Zhang, F.; Gong, G.; Li, X. Influence of initial state of magnetic suspended rotor on drop to emergency bearing. *Electromech. Eng. Technol.* **2021**, *50*, 126–129+154.
3. Kärkkäinen, A.; Sopanen, J.; Mikkola, A. Dynamic simulation of a flexible rotor during drop on retainer bearings. *J. Sound Vib.* **2007**, *306*, 601–617. [CrossRef]
4. Cao, J.; Paul, A.; Timothy, D.; Saeid, D. Auxiliary bearing system optimization for amb supported rotors based on rotor drop analysis—Part I: Rotor drop analysis method. Asme turbo expo: Turbine technical conference and exposition. *Am. Soc. Mech. Eng.* **2016**, *49835*, V07AT30A002.
5. Yu, C.; Xu, L.; Jiang, P.; Jin, C.; Zhu, Y. Rotation speed distribution ratio of double-layer rolling bearings. *J. Nanjing Univ. Aeronaut. Astronaut.* **2012**, *44*, 285–289.
6. Jiang, J.; Chen, Y. Rotor and Stator rubbing Study of nonlinear dynamics. *Adv. Mech.* **2013**, *43*, 132–148.
7. Xia, J. Research on Performance of Protective Bearing Based on Four-point Contact Ball Bearing. *Nanjing Univ. Aeronaut. Astronaut.* **2019**, *128*, 203–209.
8. Wei, P.; Wang, Y.; Yang, Y. Research on Impact Force of High-speed Suspended Rotor Falling on Protective Bearing. *Vib. Shock.* **2018**, *37*, 251–258.
9. Yu, C.; Sun, Y.; Wang, H.; Shan, W.; Chen, Y.; Qiu, R. Dynamic analysis of magnetic bearing rotor dropping on radial and axial integrated auxiliary bearing. *Mech. Mach. Theory* **2019**, *140*, 622–640. [CrossRef]
10. Sopanen, J.; Mikkola, A. Dynamic model of a deep-groove ball bearing including localized and distributed defects. Part 2: Implementation and results. Proceedings of the Institution of Mechanical Engineers, Part K. *J. Multi-Body Dyn.* **2003**, *217*, 213–223.
11. Zhu, Y.; Jin, C.; Xu, L. Dynamic Responses of Rotor Drops onto Double-decker Catcher Bearing. *Chin. J. Mech. Eng.* **2013**, *26*, 104–113. [CrossRef]
12. Castano, F.; Cruz, Y.J.; Villalonga, A.; Haber, R.E. A Data-Driven Insights on Time-to-Failure of Electromechanical Manufacturing Devices: A Procedure and Case Study. *IEEE Trans. Ind. Inform.* **2023**, *19*, 7190–7200. [CrossRef]
13. Zhu, Y.; Xu, L. Dynamic Characteristics of Bearing Protected by Elastic Ring. *J. Mech. Eng.* **2011**, *47*, 49–57.
14. Yu, C.; Xu, L.; Zhu, Y.; Jin, C. Auto-Eliminating Clearance Auxiliary Bearing Device for Active Magnetic Bearing Systems. *Tribol. Trans.* **2014**, 57. [CrossRef]
15. Muszynska, A. *Rotor-to-Stationary Part Rubbing Contact in Rotating Machinery*; CRC Press: Boca Raton, FL, USA, 2005; Chapter 5.
16. Jones, A.B. A General Theory for Elastically Constrained Ball and Radial Roller Bearings Under Arbitrary Load and Speed Conditions. *Trans. Asme* **1960**, *82*, 309. [CrossRef]

17. Mohammed, W.M.; Nejman, M.; Castano, F.; Martinez Lastra, J.L.; Strzelczak, S.; Villalonga, A. Training an Under-actuated Gripper for Grasping Shallow Objects Using Reinforcement Learning. In Proceedings of the 2020 IEEE Conference on Industrial Cyberphysical Systems, ICPS 2020, Tampere, Finland, 10–12 June 2020. [CrossRef]
18. Kingsbury, E.P. Ball motion in angular contact bearings. *Wear* **1968**, *11*, 41–50. [CrossRef]
19. Kingsbury, E.P. Torque variations in instrument ball bearings. *ASLE Trans. Wear* **1966**, *9*, 406. [CrossRef]
20. Zheng, L.; Zhu, D. Slip Analysis of High Speed Roller Bearing. *Lubr. Eng.* **1982**, *4*, 3–8.
21. Liu, Y.; Deng, Z.; Sang, D. High Speed Dynamic Performance of Cylindrical Roller Bearing with V-shaped pocket. *Acta Aeronaut. Sin.* **2021**, *42*, 579–590.
22. Maslen, E.H.; Schweitzer, G.; Bleuler, H. *Magnetic Bearings—Theory, Design, and Application to Rotating Machinery*; Springer: Berlin/Heidelberg, Germany, 2009.
23. Jiang, J.; Ulbrich, H. Derivation of coefficient of friction at high sliding speeds from energy conservation over the frictional interface. *Wear* **2001**, *247*, 66–75. [CrossRef]
24. Kuncoro, C.B.D.; Oscar, R.; Liu, C.C.; Chen, C.Y.; Hung, K.S.; Kuan, Y.D. Modeling, Analysis, and Simulation of Auxiliary Bearing for High-speed Rotating Machinery. *Sens. Mater. Int. J. Sens. Technol.* **2021**, *10 Pt 2*, 33. [CrossRef]
25. Sun, G. Auxiliary Bearing Life Prediction Using Hertzian Contact Bearing Model. *J. Vib. Acoust.* **2006**, *128*, 203–209. [CrossRef]
26. Deng, H.; Shi, Z.; Mo, N.; Sun, Z.; Zhao, J.; Liu, X. Research on on-line degradation evaluation of Electromagnetic Bearing Protection. *At. Energy Sci. Technol.* **2022**, *56*, 200–210.
27. Ma, L.; Wang, S.; Wang, P. Research on the Dynamic Characteristics of Magnetic Bearing-rotor System with Auxiliary Bearing. *J. Phys. Conf. Ser.* **2020**, *1637*, 012140. [CrossRef]
28. Sopanen, J.; Mikkola, A. Dynamic Model of a Deep Groove Ball Bearing Including Localized and Distributed Defects, Part 1: Theory. *Proc. Inst. Mech. Eng. Part K J. Multi-Body Dyn.* **2003**, *217*, 201–211. [CrossRef]
29. Ebrahimi, R.; Ghayour, M.; Khanlo, H.M. Nonlinear dynamic analysis and experimental verification of a magnetically supported flexible rotor system with auxiliary bearings. *Mech. Mach. Theory* **2018**, *121*, 545–562. [CrossRef]
30. Yu, C.; Jin, C.; Yu, X.; Xu, L. Dynamic Analysis of Active Magnetic Bearing Rotor Dropping on Auto-eliminating Clearance Auxiliary Bearing Devices. *J. Eng. Gas Turbines Power* **2015**, *137*, 062502.1–062502.14. [CrossRef]

Disclaimer/Publisher's Note: The statements, opinions and data contained in all publications are solely those of the individual author(s) and contributor(s) and not of MDPI and/or the editor(s). MDPI and/or the editor(s) disclaim responsibility for any injury to people or property resulting from any ideas, methods, instructions or products referred to in the content.